Croatian Society for Materials Protection

Metalurgija/Metallurgy

Vol. 65 No. 2 / 2026

Effect of Thermal Aging Parameters on Microstructure and Properties of 6061 Aluminum Alloy in Roller-Skating shoe Tool Holder

Liangzhu Zhang [1,*]

https://doi.org/10.64486/m.65.2.3

[1] Changchun Normal University, No.677 Changji North Line, Changchun City, Jilin Province, China, 130032, zhangliangzhu@ccsfu.edu.cn
* Correspondence: zhangliangzhu@ccsfu.edu.cn; Tel.: +8618088618688

Type of the Paper: Article
Received: August 31, 2025
Accepted: November 4, 2025

Abstract: As an important load-bearing structure of roller-skating shoes, the tool holder is mostly made of metal. 6061 aluminum alloy is widely used in the manufacture of roller-skating shoe tool holders because of its high strength, good formability, and strong corrosion resistance. To achieve higher strength after plastic forming, heat treatment, such as solution treatment and aging is usually required. In this study, 6061 solution-treated aluminum alloy was used as the research material. It was found that during the thermal aging process, the hardness of the alloy first increased to a peak value and then decreased to a stable value. At an aging temperature of 170 °C, the peak hardness reached 128.4 HV after 120 min. The average residual stress release rate at three positions of the 6061 aluminum alloy was about 37 %. After 180 min, the hardness decreased again to its lowest value and tended to stabilize, while the average residual stress release rate increased to 50 %. The experimental results provide theoretical guidance for optimizing the processing of 6061 aluminum alloy in the manufacture of roller-skating shoe tool holders.

Keywords: roller skates; 6061 aluminum alloy; thermal aging; alloy hardness

1. Introduction

As a typical Al–Mg–Si series heat-treatable strengthening alloy, 6061 aluminum alloy has been widely used in aerospace, transportation, and sports equipment (such as roller-skating shoe tool holders) due to its excellent strength–ductility balance, corrosion resistance, and formability [1–3].

As the core load-bearing component, the roller-skating shoe tool holder must meet the requirements of both light weight and high structural stability. Lightweight design reduces skating energy consumption, while structural stability depends on the effective control of residual stress within the material and the accurate matching of mechanical properties [4–5]. At present, the performance of 6061 aluminum alloy in industrial production is optimized through a "solution + aging" process. Thermal aging is the key stage that determines the strengthening effect and stress release efficiency. The selection of its parameters (temperature and time) directly affects the precipitation behavior (nucleation, growth, and coarsening) of the Mg_2Si strengthening phase in the alloy and the evolution of residual stress [6–10].

Although the aging hardening characteristics of 6061 aluminum alloy have been clarified in previous studies for example, increasing the aging temperature accelerates the precipitation of the Mg_2Si phase and shortens the time to reach peak hardness [10–13], there are still notable gaps regarding 6061 aluminum alloy used for roller-skating shoe tool holders. On the one hand, most studies focus on alloys used in aviation or automotive applications (where the service environment is mainly high temperature and high load), whereas the roller-skating tool holder is subjected to periodic impact loads during service, requiring a higher uniformity of residual stress distribution. Existing research has not specifically analyzed the stress release differences at various positions within a specific structural sample (such as a thin-gauge sheet prototype of the tool holder). On the other hand, most studies discuss separately the effects of aging parameters on hardness or residual stress and lack a systematic analysis of the correlation between the two, such as whether the stress release rate at the peak hardness state meets the dimensional stability requirements of the tool holder, or whether the aging state corresponding to high stress release efficiency results in an excessive decrease in hardness. These key issues remain unresolved [13–18].

In addition, there is still debate regarding the mechanism of residual stress evolution during the aging process of 6061 aluminum alloy. Some scholars suggest that the release of residual stress mainly depends on dislocation slip induced by atomic thermal motion [19], while others argue that the precipitation of the Mg_2Si phase produces local internal stress that may either inhibit or promote stress release, depending on the size and distribution of the precipitated phases [20–21]. For thin 6061 aluminum alloy components (such as those used in roller-skating shoe tool holders with a thickness of about 2 mm), the competition between these mechanisms has not yet been fully clarified. Therefore, in this study, the effects of thermal aging parameters (170 °C–210 °C, 0 min–180 min) on the microstructure, hardness, and residual stress of cold-rolled 6061 aluminum alloy were systematically investigated, and the correlation between the stress release behavior and hardness evolution at different positions was analyzed. The purpose of this study is to provide theoretical support and an experimental basis for optimizing the heat treatment process of 6061 aluminum alloy used in roller-skating shoe tool holders.

2. Materials and Methods

2.1 Material pretreatment

The raw material used in this experiment was cold-rolled 6061 aluminum alloy in the industrial-grade cold-rolled supply state. After the cold rolling process, a certain degree of work hardening occurred within the material, and the grains exhibited a preferred orientation, providing a structural basis for the subsequent solution-aging treatment. The specific chemical composition (mass fraction, %) of the 6061 aluminum alloy is shown in Table 1 below.

Table 1. Chemical composition of 6061 aluminum alloy

Element	Si	Mg	Cu	Mn	Fe	Zn	Ti	Al
Mass fraction / %	0.5135	0.8348	0.1929	0.0288	0.3443	0.0081	0.0293	Bal.

The cold-rolled 6061 aluminum alloy was processed into two types of samples for microstructure and hardness testing. The rectangular samples (200 mm × 50 mm × 2 mm) ensured that the test area was sufficiently representative. For residual stress testing, circular samples with a diameter of 15 mm and a thickness of 2 mm were prepared to facilitate directional measurement of residual stress at specific positions. The flatness error of each sample was controlled within 0.02 mm to avoid the influence of shape deviation on the residual stress results. After machining, all samples were polished sequentially using 400#–1200# sandpaper to remove surface oxide layers and machining burrs, then ultrasonically cleaned in anhydrous ethanol for 15 min to remove surface oil contamination, and finally dried for later use.

https://doi.org/10.64486/m.65.2.3

To obtain a single-phase supersaturated solid solution state in 6061 aluminum alloy and to establish a basis for precipitation strengthening in the subsequent thermal aging process, a controllable residual stress was introduced during the solution treatment. The specific parameters were as follows: the solution treatment temperature was 530 °C, the holding time was 1 h, the quenching medium was water, and the transfer time during quenching was less than 5 s. The temperature of 530 °C was selected because it ensures that Mg, Si, and other alloying elements are fully dissolved in the Al matrix to form a uniform supersaturated solid solution while avoiding excessive grain growth that could occur at higher temperatures (above approximately 550 °C). This temperature therefore balances the effects of solution treatment and matrix grain refinement. Moreover, 530 °C is within the control capability of a conventional box-type electric furnace, without requiring special high-temperature equipment. A holding time of 1 h is sufficient for complete dissolution of alloying elements. This process is cost-effective and efficient, meeting the adaptability requirements for large-scale production of roller-skating shoe tool holders.

2.2 Experimental methods

The solution treatment and thermal aging of the aluminum alloy were carried out in an SXL-1200C box-type experimental electric furnace. The internal dimensions of the furnace were 160 × 150 × 150 mm, and the temperature control accuracy was ±1 °C. The thermal aging temperature range was set from 170 °C to 210 °C, including three gradient temperatures of 170 °C, 190 °C, and 210 °C. The thermal aging duration ranged from 0 min to 180 min, with specific sampling time points at 0 min (solution-treated state), 30 min, 60 min, 90 min, 100 min, 120 min, 150 min, and 180 min. To ensure experimental repeatability and data reliability, three parallel samples were prepared for each thermal aging condition. Subsequent hardness and residual stress tests were conducted on these three parallel samples, and the final results were averaged to minimize the influence of random errors on the experimental conclusions.

The hardness of the samples was measured using the Vickers hardness testing method (HV) on an HVS-1000 digital display Vickers hardness tester. Five evenly distributed test points were selected on each sample, and all five hardness readings were recorded. Abnormal values (deviations exceeding ±5 % from the average) were excluded, and the mean value of the remaining measurements was taken as the hardness of the sample. The average hardness of the three parallel samples was then calculated to obtain the final hardness result for each thermal aging condition, ensuring accuracy and representativeness of the data. Residual stress was measured using X-ray diffraction (XRD). Three characteristic positions were selected on each circular sample for testing by an X-ray diffractometer. At each position, the residual stress was measured only in the direction perpendicular to the sample's radial direction, and each measurement was repeated three times. Before each measurement, the sample was precisely repositioned to ensure that the positional deviation of the measurement point did not exceed 0.1 mm. Microstructural characterization was performed using transmission electron microscopy (TEM) to observe the microstructural evolution of the alloy during thermal aging. For TEM analysis, 10 mm × 10 mm sheets were cut from samples subjected to different thermal aging treatments, and the morphology, size, and distribution characteristics of the precipitated phases were observed and recorded.

3. Results

The microstructure of the aluminum alloy after thermal aging at 170 °C was analyzed using transmission electron microscopy (TEM). Figure 1 shows the corresponding TEM observations. It can be clearly seen that, under the thermal aging treatment, various forms of precipitates are uniformly distributed throughout the aluminum alloy matrix, mainly including needle-shaped, rod-shaped, and a small number of spherical structures. Figure 1a shows the bright-field TEM image of the aluminum alloy at the peak hardness state when the thermal aging time was 120 min. At this stage, the matrix is filled with a high density of fine precipitates [22–23]. These needle-shaped and rod-shaped precipitates, with their uniform and dense dispersion, provide a significant precipitation strengthening effect for the 6061 aluminum alloy by hindering dislocation movement.

After further prolonging the thermal aging time to 180 min, as shown in Figure 1b, although the number density of the precipitates decreases slightly, their average size increases to some extent compared with the

https://doi.org/10.64486/m.65.2.3

120 min aging condition. However, no rapid coarsening phenomenon occurs, and the overall distribution pattern remains relatively uniform.

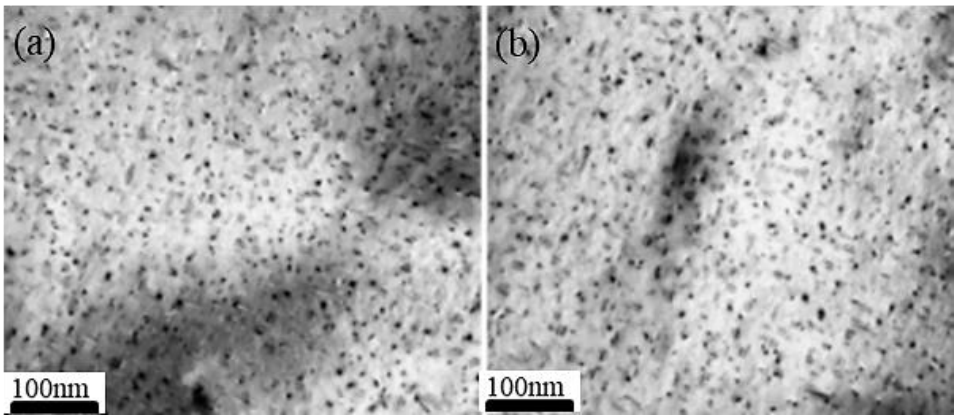

Figure 1. TEM bright-field images of 6061 aluminum alloy aged at 170 °C: (a) 120 min; (b) 180 min.

To determine the type of precipitated phases formed after thermal aging treatment, the microstructure of the precipitates was analyzed by high-resolution transmission electron microscopy (HRTEM). Figure 2 shows the HRTEM images and the corresponding fast Fourier transform (FFT) patterns obtained after thermal aging. Figure 2a presents the HRTEM image of the sample aged for 120 min (peak aging condition). Based on the diffraction spots obtained from the FFT, the precipitated phase was identified as belonging to the monoclinic crystal system, with lattice parameters a = 1.51 nm, c = 0.67 nm, and β = 105° . This indicates that the precipitate is the β' phase, corresponding to the precipitates observed in Figure 1a. After aging for 180 min, the precipitated phase was also identified as β' (a = b = 0.71 nm, γ = 120°), as shown in Figure 2c, corresponding to the precipitates observed in Figure 1b. It can be seen that, during thermal aging from 120 min to 180 min, the change in the size and density of the precipitates is mainly attributed to the evolution of the β' phase.

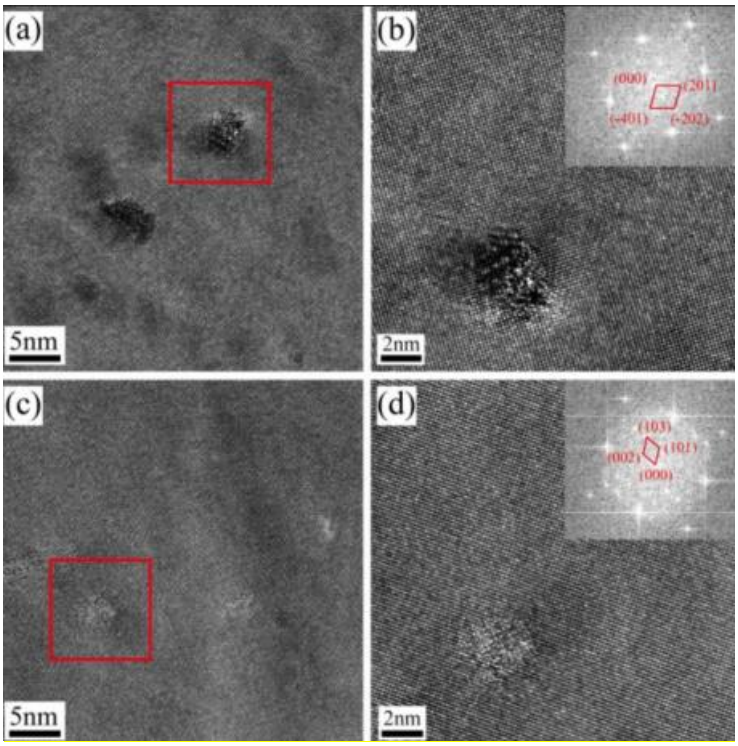

Figure 2. HRTEM images and corresponding fast Fourier transform (FFT) patterns of 6061 aluminum alloy: (a, b) aged at 180 °C for 120 min; (c, d) aged at 180 °C for 180 min.

https://doi.org/10.64486/m.65.2.3

In this study, the effects of thermal aging parameters—namely temperature and time—on the hardness of solution-treated 6061 aluminum alloy were investigated. The results are shown in Figure 3. It can be seen from the figure that during the thermal aging process, the hardness variation of the alloy at different temperatures follows a similar trend. With increasing aging time, the hardness of the aluminum alloy first rises to a peak value and then decreases, eventually reaching a stable level. However, different thermal aging temperatures lead to variations in the kinetics of hardening [24–26]. As the thermal aging temperature increases, the time required to reach the peak hardness of the aluminum alloy becomes significantly shorter, while the corresponding peak hardness value decreases [27]. At 170 °C, the alloy reaches the highest hardness of 128.4 HV after 120 min. At 190 °C, the maximum hardness of 119.1 HV occurs after 100 min, while at 210 °C, the maximum hardness of 113.2 HV is reached after 47 min. Compared with the solution-treated state (57 HV), the peak hardness values at different thermal aging temperatures are higher by 71.4 HV, 62.1 HV, and 56.2 HV, respectively. The specific results are summarized in Table 2. When the aging time was extended to 180 min, the hardness of the aluminum alloy gradually decreased, reaching 107.1 HV, 98.5 HV, and 93.3 HV for 170 °C, 190 °C, and 210 °C, respectively.

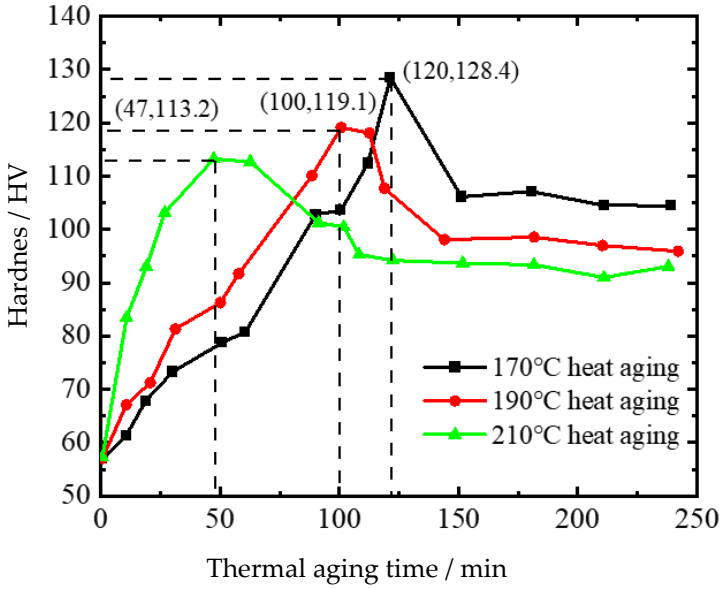

Figure 3. Relationship between thermal aging time and hardness of 6061 aluminum alloy at 170 °C, 190 °C, and 210 °C.

Table 2. Peak hardness and corresponding time of 6061 solid solution aluminum alloy at different thermal aging temperatures.

Thermal aging temperature / °C	Peak hardness time / min	maximum hardness / HV
170	120	128.4
190	100	119.1
210	47	113.2

The variation of residual stress in solution-treated 6061 aluminum alloy during thermal aging at 170 °C was investigated. It should be noted that, to obtain the residual stress distribution at different locations, each circular aluminum alloy specimen was tested at three positions, and at each position the stress was measured in one direction, perpendicular to the radius of the circle as illustrated in Figure 4. As shown in Figure 5, after solution quenching, the internal residual stress of the 6061 aluminum alloy circular specimen is compressive (negative value) in the direction perpendicular to the radius. During thermal aging at 170 °C, the variation in

https://doi.org/10.64486/m.65.2.3

residual stress does not show a simple monotonic decrease but differs significantly depending on the test position. Among them, the absolute value of residual stress increases at the inner position (II) when the aging time reaches 120 min. This may be attributed to the initially lower residual stress at position II in the solution-treated state, while the initial stress at the center (I) and outer (III) positions is higher. In the early stage of thermal aging (0–120) min, the stress at positions I and III is rapidly released and transferred toward the inner position II, due to enhanced atomic thermal motion. This leads to local stress accumulation at position II, manifested as an increase in the absolute value of compressive residual stress.

After solution treatment, the maximum residual stress in the aluminum alloy sample appears at the center position (I), reaching −110.6 MPa, while the minimum residual stress is observed at the inner position (II), with a value of −35.9 MPa. After thermal aging for 180 min, compared with the solution-treated state, the residual stresses at the center (I) and outer (III) positions decreased significantly by 74.6 MPa and 58.4 MPa, respectively, relative to their initial values of −110.6 MPa and −82.9 MPa. The residual stress at the inner position (II) first increased and then decreased. After 120 min of thermal aging, the residual stress at position II increased from −35.9 MPa to −59.4 MPa, representing an increase of approximately 65 %. Although partial stress relaxation occurred after 180 min, the residual stress decreased by only 5.1 MPa, and the final residual stress at position II remained higher than the initial stress in the solution-treated state. These results indicate that, during thermal aging, the residual stresses at the center (I) and outer (III) positions of the aluminum alloy decrease much more rapidly than at the inner position (II). The overall stress relaxation thus mainly occurs through the inner and outer regions of the sample.

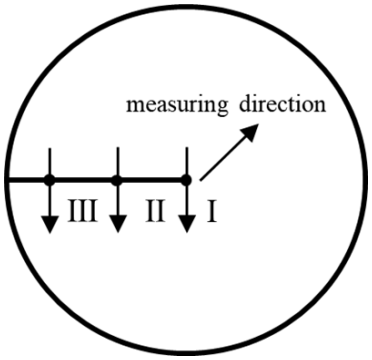

Figure 4. Schematic diagram of residual stress measurement positions I, II, and III.

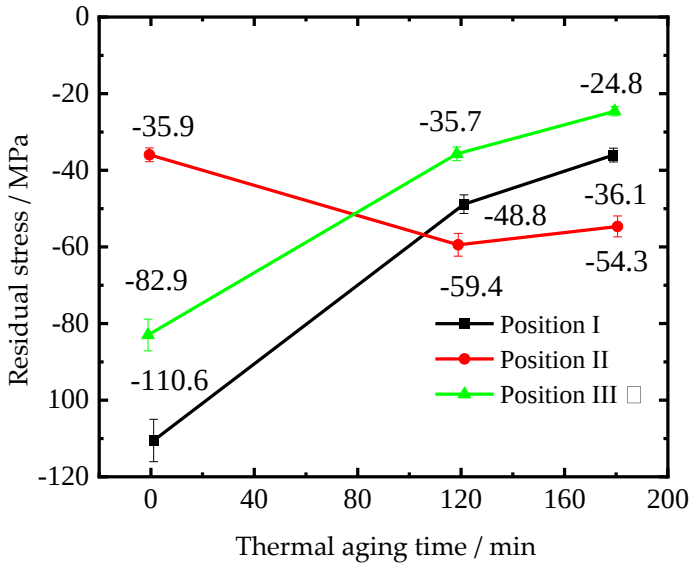

Figure 5. Relationship between aging time and residual stress of 6061 aluminum alloy at 170 °C.

https://doi.org/10.64486/m.65.2.3

Table 3 presents the mean and standard deviation values of residual stress for aluminum alloy samples at different stages of solution treatment and thermal aging. It can be observed that, compared with the solution-treated state, both the mean residual stress and its standard deviation decrease significantly after thermal aging. After thermal aging, the average residual stress of the aluminum alloy decreased from −76.5 MPa to −38.4 MPa, representing a reduction of 50 %. The maximum standard deviation decreased from 38.0 MPa to 15.2 MPa, corresponding to a 60 % reduction. These results indicate that the residual stress distribution within the aluminum alloy becomes more uniform after thermal aging. When comparing the residual stress relaxation rate with the change in hardness during thermal aging at 170 °C, it was found that the peak hardness of the 6061 aluminum alloy occurred after 120 min, reaching 128.4 HV. After 180 min of aging, the hardness decreased and stabilized at approximately 113.2 HV, while the average residual stress relaxation rate reached 50 %. Overall, during thermal aging, the hardness of the aluminum alloy first increases and then decreases, while the average residual stress release rate across the three measurement positions gradually declines.

Table 3. Mean value and standard deviation of residual stress at different time of thermal aging.

Measuring direction	Solid solution state		Thermal aging 120 min		Thermal aging 180 min	
	Mean value MPa	St. dev. MPa	Mean value MPa	St. dev MPa	Mean value MPa	St. dev. MPa
Vertical to the radius of the circle	-76.5	38	-47.9	11.8	-38.4	15.2

4. Discussion

The results of this study provide valuable insights into the effects of thermal aging parameters on the microstructure and properties of 6061 aluminum alloy, particularly in the context of its application as a roller-skating shoe tool holder. The observed changes in hardness and residual stress during the thermal aging process can be attributed to the precipitation of strengthening phases and the evolution of residual stress distribution within the alloy.

During the thermal aging process, the hardness of the 6061 aluminum alloy initially increases to a peak value before gradually decreasing to a stable level. This behavior is consistent with the precipitation hardening mechanism, where fine precipitates form and strengthen the alloy matrix. The residual stress distribution within the alloy also evolves during thermal aging. The initial compressive residual stress generated during the solution treatment and quenching process is significantly reduced as the aging time increases.

The residual stress at the center and outer positions of the alloy sample decreases more rapidly compared to the inner position, suggesting that the residual stress is primarily released from the outer and inner sides of the sample. The relationship between hardness and residual stress release rate during thermal aging is noteworthy. The peak hardness corresponds to a significant release of residual stress, indicating that the formation of fine precipitates not only enhances the alloy's hardness but also contributes to the relaxation of residual stress. As the aging time progresses, the hardness decreases, and the residual stress release rate also slows down, suggesting a correlation between the two properties. This correlation highlights the importance of optimizing thermal aging parameters to achieve a balance between hardness and residual stress reduction.

In conclusion, the thermal aging process significantly influences the microstructure and properties of 6061 aluminum alloy. The findings of this study emphasize the importance of carefully selecting thermal aging parameters to optimize the alloy's mechanical properties and residual stress distribution. These insights provide a theoretical basis for the production of high-strength and stable 6061 aluminum alloy roller-skating shoe tool holders, contributing to the advancement of materials science in this specific application. Future research may focus on exploring additional heat treatment parameters and their effects on other mechanical properties, such

https://doi.org/10.64486/m.65.2.3

as tensile strength and fatigue resistance, to further enhance the performance of 6061 aluminum alloy in demanding applications.

5. Conclusions

In this study, the effects of thermal aging on the hardness, residual stress, and microstructure of solution-treated 6061 aluminum alloy were investigated, and the mechanisms of precipitate formation and residual stress evolution were analyzed in relation to hardness behavior. The main conclusions are as follows:

1. During the thermal aging process, the hardness of the aluminum alloy first increases to a peak value and then gradually decreases to a stable level. Both the time required to reach peak hardness and the peak hardness value are affected by the thermal aging temperature. With increasing aging temperature, the time to reach the peak hardness is shortened, while the corresponding peak hardness gradually decreases. At 170 °C, the aluminum alloy reaches the highest hardness value of 128.4 HV after 120 min.
2. During thermal aging, the residual stress at the center (I) and outer (III) positions of the aluminum alloy decreases rapidly, significantly more than at the inner (II) position. This indicates that residual stress is mainly released through the outer and inner regions of the sample. Meanwhile, the average residual stress relaxation rate at all three positions increases with time, contributing to a more stable aluminum alloy structure.

References

[1] T. Losnegard *et al.*, "Test–retest reliability of performance variables during treadmill rollerski skating," *Eur. J. Appl. Physiol.*, vol. 125, no. 7, pp. 1–7, 2025, Available: https://link.springer.com/article/10.1007/s00421-025-05746-w

[2] A. Rebelo *et al.*, "Validity of a wearable device for measuring vertical displacement and jump count in young artistic roller skating athletes," *Proc. Inst. Mech. Eng. Part P: J. Sports Eng. Technol.*, vol. 239, no. 1, pp. 53–60, 2025, https://doi.org/10.1177/17543371231188400

[3] G. Bongiorno *et al.*, "The kinematic and electromyographic analysis of roller skating at different speeds on a treadmill: A case study," *Sensors*, vol. 24, no. 17, p. 5738, 2024, https://doi.org/10.3390/s24175738

[4] M. M. Dhodapkar *et al.*, "Orthopaedic injury patterns related to ice skating, inline skating, and roller skating: A 20-year epidemiologic analysis," *Orthop. J. Sports Med.*, vol. 11, no. 9, p. 23259671231198208, 2023, https://doi.org/10.1177/23259671231198208

[5] N. Zhou *et al.*, "The effect of direct quenching on the microstructure and mechanical properties of NiCrMo and Cu-bearing high-strength steels," *Materials*, vol. 17, no. 6, 2024, https://doi.org/10.3390/ma17061397

[6] M. N. Ahmad Fauzi, M. B. Uday, H. Zuhailawati, and A. B. Ismail, "Microstructure and mechanical properties of alumina-6061 aluminum alloy joined by friction welding," Materials & Design, vol. 31, no. 2, pp. 670–676, Feb. 2010, https://doi.org/10.1016/j.matdes.2009.08.019.

[7] F. Picasso and E. Paiva, "Training and proprietary equipment: The bow and the arrow to shoot the target," *RAUSP Manag. J.*, vol. 60, no. 1, pp. 102–122, 2025, https://doi.org/10.1108/RAUSP-06-2023-0105

[8] D. Liu *et al.*, "Semi-solid die forging process for the 6061-aluminum rim support disc," *Proc. Inst. Mech. Eng. Part C: J. Mech. Eng. Sci.*, vol. 239, no. 14, pp. 5452–5464, 2025, https://doi.org/10.1177/09544062251328887

[9] R. F. Escamilla *et al.*, "Effects of step length and stride variation during forward lunges on lower-extremity muscle activity," *J. Funct. Morphol. Kinesiol.*, vol. 10, no. 1, p. 42, 2025, https://doi.org/10.3390/jfmk10010042

[10] S.-J. Lee, M.-S. Han, and S.-J. Kim, "The Effects of Maintaining Temperature in Annealing Heat Treatment for an FSWed 6061-T6 Al Alloy," Microscopy and Microanalysis, vol. 19, no. S5, pp. 69–72, Aug. 2013, https://doi.org/10.1017/s1431927613012361

[11] W. Liu *et al.*, "The effects of heat treatment on microstructure and mechanical properties of selective laser melting 6061 aluminum alloy," *Micromachines*, vol. 13, no. 7, p. 1059, 2022, https://doi.org/10.3390/mi13071059

 https://doi.org/10.64486/m.65.2.3

[12] A. N. A. Alfaqeer *et al.*, "Influence of annealing temperature variations on the structural, morphological, optical and electrical properties of Ge35Se65 thin films," *J. Electron. Mater.*, vol. 54, no. 6, pp. 1–11, 2025, https://doi.org/10.1007/s11664-025-11890-y

[13] J. Wu *et al.*, "Influence of annealing temperatures on the properties of Gd_2O_2S:Tb scintillation ceramics for neutron imaging," *Opt. Mater.*, vol. 162, p. 116860, 2025, https://doi.org/10.1016/j.optmat.2025.116860

[14] R. Wang *et al.*, "Fatigue performance of 7075/6061 dissimilar aluminum alloy TIG welds," *J. Mech. Sci. Technol.*, vol. 39, no. 8, pp. 1–6, 2025, Available: https://link.springer.com/article/10.1007/s12206-025-0714-3

[15] B. He *et al.*, "Microstructure and mechanical properties of wear-resistant SiCp/Al composite layers on 6061 aluminum alloy fabricated by additive friction stir deposition," *Addit. Manuf.*, vol. 109, p. 104880, 2025, https://doi.org/10.1016/j.addma.2025.104880

[16] H. Zhou *et al.*, "Axial compression bearing performance of large-scale explosively welded TA10 titanium alloy/6061 aluminum alloy composite pipes," *Thin-Walled Struct.*, vol. 216, p. 113629, 2025, https://doi.org/10.1016/j.tws.2025.113629

[17] Y.-L. Ding *et al.*, "Effect of annealing temperature on joints of diffusion bonded Mg/Al alloys," *Trans. Nonferrous Met. Soc. China*, vol. 28, no. 2, pp. 251–258, 2018, https://doi.org/10.1016/S1003-6326(18)64658-8

[18] H. Zhou *et al.*, "Effect of laser power on microstructure and micro-galvanic corrosion behavior of 6061-T6 aluminum alloy welding joints," *Metals*, vol. 11, no. 1, p. 3, 2020, https://doi.org/10.3390/met11010003

[19] P. Huang *et al.*, "Achieving highly dense metal injection moulding 6061 Al with superior strength-ductility," *Mater. Sci. Eng. A*, vol. 943, p. 148827, 2025, https://doi.org/10.1016/j.msea.2025.148827

[20] H. Zhou *et al.*, "Effect of laser power on hybrid laser–gas metal arc welding (GMAW) of a 6061 aluminum alloy," *J. Korean Phys. Soc.*, vol. 77, no. 11, pp. 991–996, 2020, https://doi.org/10.3938/jkps.77.991

[21] T. Wu *et al.*, "Deformation and microstructural evolution behavior of pre-hardened 6061 aluminum alloy during static tensile process," *Mater. Charact.*, vol. 227, p. 115319, 2025, https://doi.org/10.1016/j.matchar.2025.115319

[22] K. Zhu et al., "Effect of rapid heat treatment on mechanical properties and precipitation behavior of medium carbon low alloy steel," Journal of Materials Research and Technology, vol. 35, pp. 5730–5745, Feb. 2025, doi: https://doi.org/10.1016/j.jmrt.2025.02.206

[23] Y. Li, Z. Liu, Q. Xia, S. Bai, and X. Chen, "Effects of aging temperature on the precipitation behavior of Ω phase in an Al-Cu-Mg-Ag alloy," Metals and Materials International, vol. 17, no. 1, pp. 1–6, Feb. 2011, doi: https://doi.org/10.1007/s12540-011-0201-5

[24] P. Liang et al., "Aging precipitation behavior and strengthening mechanisms of 6061 aluminum alloy with a bimodal heterostructure," Results in Engineering, pp. 106653–106653, Aug. 2025, doi: https://doi.org/10.1016/j.rineng.2025.106653

[25] K. Huang et al., "Effect of quenching cooling rate on residual stress and microstructure evolution of 6061 aluminum alloy," Journal of Central South University, vol. 31, no. 7, pp. 2167–2180, Jul. 2024, https://doi.org/10.1007/s11771-024-5705-5

[26] M. Benachour, N. Benachour, and M. Benguediab, "Effect of compressive residual stress generated by plastic preload on fatigue initiation of 6061 Al-alloy," Procedia Structural Integrity, vol. 2, pp. 3090–3097, 2016, doi: https://doi.org/10.1016/j.prostr.2016.06.386

[27] M. Kaseem, M. P. Kamil, J. H. Kwon, and Y. G. Ko, "Effect of Sodium Benzoate on Corrosion Behavior of 6061 Al Alloy Processed by Plasma Electrolytic Oxidation," Surface & Coatings Technology, vol. 285, pp. 103–110, 2016 https://doi.org/10.1016/j.surfcoat.2015.11.006